The cold-induced lipokine 12,13-diHOME promotes fatty acid transport into brown adipose tissue

Matthew D Lynes[1], Luiz O Leiria[1], Morten Lundh[1,2], Alexander Bartelt[3], Farnaz Shamsi[1], Tian Lian Huang[1], Hirokazu Takahashi[1], Michael F Hirshman[1], Christian Schlein[3], Alexandra Lee[3], Lisa A Baer[4], Francis J May[4], Fei Gao[5], Niven R Narain[5], Emily Y Chen[5], Michael A Kiebish[5], Aaron M Cypess[6], Matthias Blüher[7], Laurie J Goodyear[1], Gökhan S Hotamisligil[3], Kristin I Stanford[4] & Yu-Hua Tseng[1,8]

Brown adipose tissue (BAT) and beige adipose tissue combust fuels for heat production in adult humans, and so constitute an appealing target for the treatment of metabolic disorders such as obesity, diabetes and hyperlipidemia[1,2]. Cold exposure can enhance energy expenditure by activating BAT, and it has been shown to improve nutrient metabolism[3–5]. These therapies, however, are time consuming and uncomfortable, demonstrating the need for pharmacological interventions. Recently, lipids have been identified that are released from tissues and act locally or systemically to promote insulin sensitivity and glucose tolerance; as a class, these lipids are referred to as 'lipokines'[6–8]. Because BAT is a specialized metabolic tissue that takes up and burns lipids and is linked to systemic metabolic homeostasis, we hypothesized that there might be thermogenic lipokines that activate BAT in response to cold. Here we show that the lipid 12,13-dihydroxy-9Z-octadecenoic acid (12,13-diHOME) is a stimulator of BAT activity, and that its levels are negatively correlated with body-mass index and insulin sensitivity. Using a global lipidomic analysis, we found that 12,13-diHOME was increased in the circulation of humans and mice exposed to cold. Furthermore, we found that the enzymes that produce 12,13-diHOME were uniquely induced in BAT by cold stimulation. The injection of 12,13-diHOME acutely activated BAT fuel uptake and enhanced cold tolerance, which resulted in decreased levels of serum triglycerides. Mechanistically, 12,13-diHOME increased fatty acid (FA) uptake into brown adipocytes by promoting the translocation of the FA transporters FATP1 and CD36 to the cell membrane. These data suggest that 12,13-diHOME, or a functional analog, could be developed as a treatment for metabolic disorders.

Cold exposure activates the uptake and utilization of metabolic fuels in BAT in as little as 1 h in humans[9]. We hypothesized that thermogenic lipokines linked to BAT activation might increase in individuals exposed to an acute cold challenge, given that both lipokines and cold exposure can have beneficial effects on metabolism[3–5,10]. To test this hypothesis, we used liquid chromatography–tandem mass spectrometry (LC–MS/MS) to measure the concentrations of a panel of 88 lipids with annotated signaling properties in the plasma of human volunteers exposed to 1 h of cold at 14 °C[9] (**Supplementary Fig. 1a,b** and **Supplementary Table 1**). This approach to identify putative lipokines is highly sensitive and covers a broad range of oxidized fatty acid metabolites. Notably, three lipid species were significantly ($P < 0.05$) increased in human circulation by cold exposure after 1 h of cold challenge (**Fig. 1a** and **Supplementary Fig. 2**). The lipid 12,13-diHOME, however, was the only species that increased in all individuals measured (**Fig. 1b**), and 12,13-diHOME concentration was correlated with BAT activity, as measured by radiolabeled glucose uptake (**Fig. 1c**).

BAT activity and its mass are both decreased with obesity[1]; thus, to determine whether 12,13-diHOME is linked to human obesity and its related metabolic disorders, we measured 12,13-diHOME in a cohort of 55 individuals at room temperature. Importantly, we found significant, negative associations between the plasma concentration of 12,13-diHOME and body-mass index (BMI), insulin resistance (as measured by the homeostatic model of insulin resistance, or HOMA-IR), fasting plasma insulin and glucose concentrations (**Fig. 1d,e** and **Supplementary Fig. 3a–c**), although there was not a statistically significant correlation between 12,13-diHOME and either hemoglobin A1c or c-reactive peptide (**Supplementary Fig. 3d,e**). In agreement with the correlation between 12,13-diHOME and BMI, we found that circulating triglyceride and leptin levels were also negatively correlated with plasma concentrations of 12,13-diHOME (**Fig. 1f** and **Supplementary Fig. 3f**). Notably, circulating triglycerides remained significantly correlated with 12,13-diHOME concentration after we accounted for BMI as a covariate in a linear model
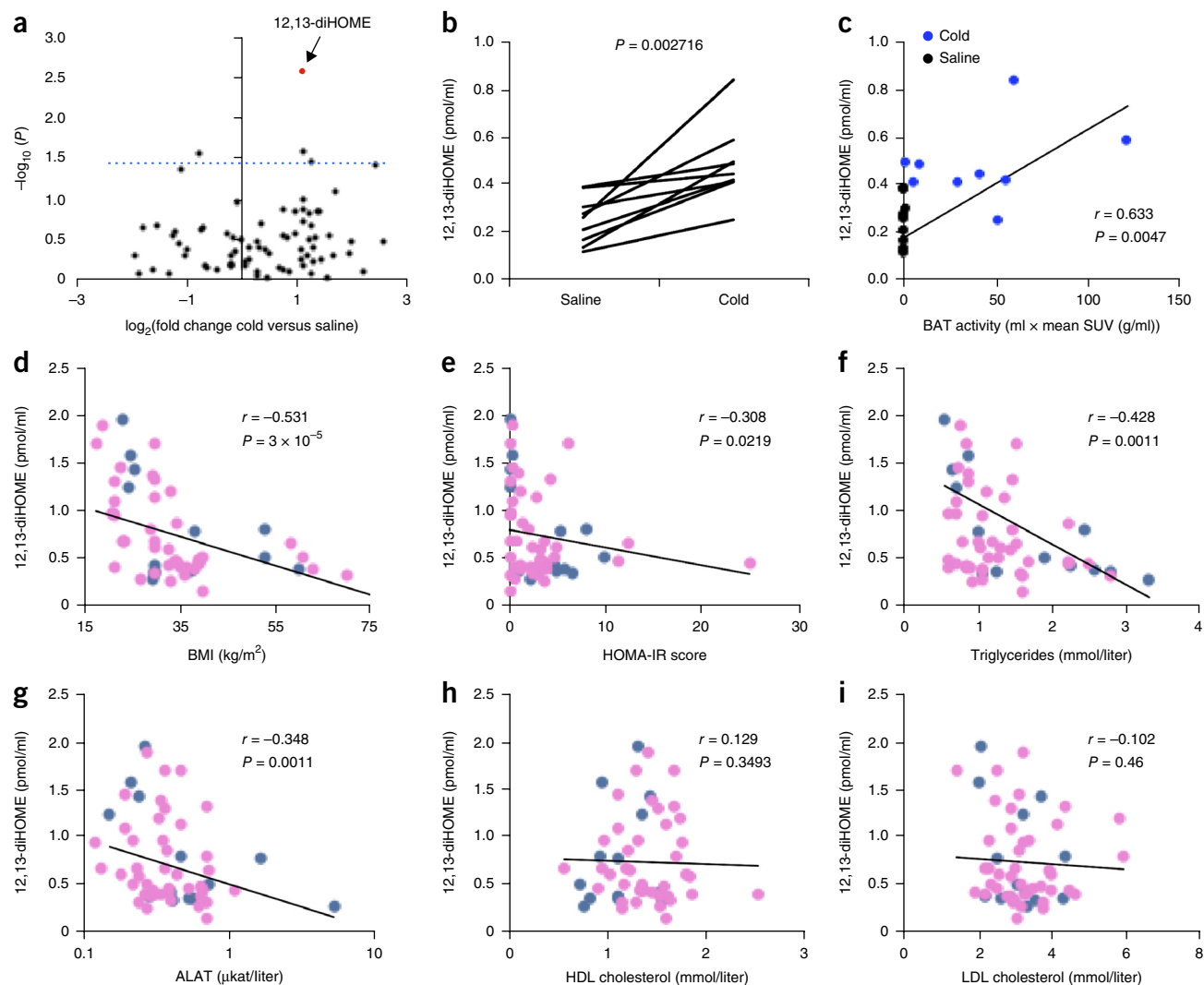
Figure 1 Discovery of 12,13-diHOME, a cold-induced lipokine linked to BAT activation. (**a**) Volcano plot of 88 lipids, comparing the fold induction after cold challenge to the *P* value (paired Student's *t*-test). The dashed line indicates a *P* value of 0.05. 12,13-diHOME is highlighted in red. *n* = 9 human subjects. (**b**) Individual plasma concentration of 12,13-diHOME before and after cold challenge. The *P* value for a paired Student's *t*-test is shown. (**c**) Plasma 12,13-diHOME concentration plotted with BAT-standardized uptake value (SUV), as measured by a positron-emission tomography (PET) scan of radiolabeled fluorodeoxyglucose. *r* is the Spearman correlation coefficient between 12,13-diHOME and BAT activity. (**d–i**) Circulating 12, 13-diHOME concentration plotted against BMI (**d**), HOMA-IR (score) (**e**), circulating triglycerides (**f**), circulating ALAT (**g**), circulating HDL cholesterol (**h**) and LDL cholesterol (**i**). Throughout, *r* is the Spearman correlation coefficient between 12,13-diHOME and each parameter. Blue dots represent males; pink dots, females. *n* = 55 individuals (13M/42F). *P* value was calculated using algorithm AS 89.

(*P* = 0.0463; **Supplementary Table 2**). Circulating markers of liver function, such as alanine transaminase (ALAT) (**Fig. 1g**), aspartate transaminase (ASAT) (**Supplementary Fig. 3g**) and γ-glutamyl transpeptidase (gGT) (**Supplementary Fig. 3h**), were inversely correlated with 12,13-diHOME concentration, and both ALAT (*P* = 0.0494) and ASAT (*P* = 0.0274) remained significantly correlated when BMI was accounted for as a covariate. Cholesterol (high-density lipoprotein (HDL), low-density lipoprotein (LDL) or total), on the other hand, was not correlated with circulating 12,13-diHOME concentration (**Fig. 1h,i** and **Supplementary Fig. 3i**). In this particular cohort of individuals, we found that circulating 12,13-diHOME had no statistically significant association with age, gender or diabetes status (**Supplementary Fig. 3i–l**).

To enable us to carry out in-depth mechanistic studies, we established a cold-exposure model, using mice housed at either 30 °C

(i.e., at thermoneutrality, at which point there is minimal BAT activity) or 4 °C (with maximal BAT activity) for various durations. Consistent with what was observed in humans, exposing mice to 4 °C for 1 h increased circulating levels of 12,13-diHOME (**Fig. 2a**). Of note, treatment of mice with norepinephrine (NE) for 30 min, which mimics sympathetic activation, also induced 12,13-diHOME production, which suggests that 12,13-diHOME is a potential product induced by both cold and sympathetic activation. Similar to acute cold challenge, 1 week of cold exposure also induced a pronounced increase in circulating 12,13-diHOME levels male mice (**Fig. 2b**). In female mice, 12,13-diHOME was not significantly changed in the circulation after 1 week of cold exposure; however, this increase did reach statistical significance after exposure to cold for 11 d (**Fig. 2b** and **Supplementary Fig. 4a**), which might be related to the reported sexual dimorphism of lipid profiles in mouse BAT[11].
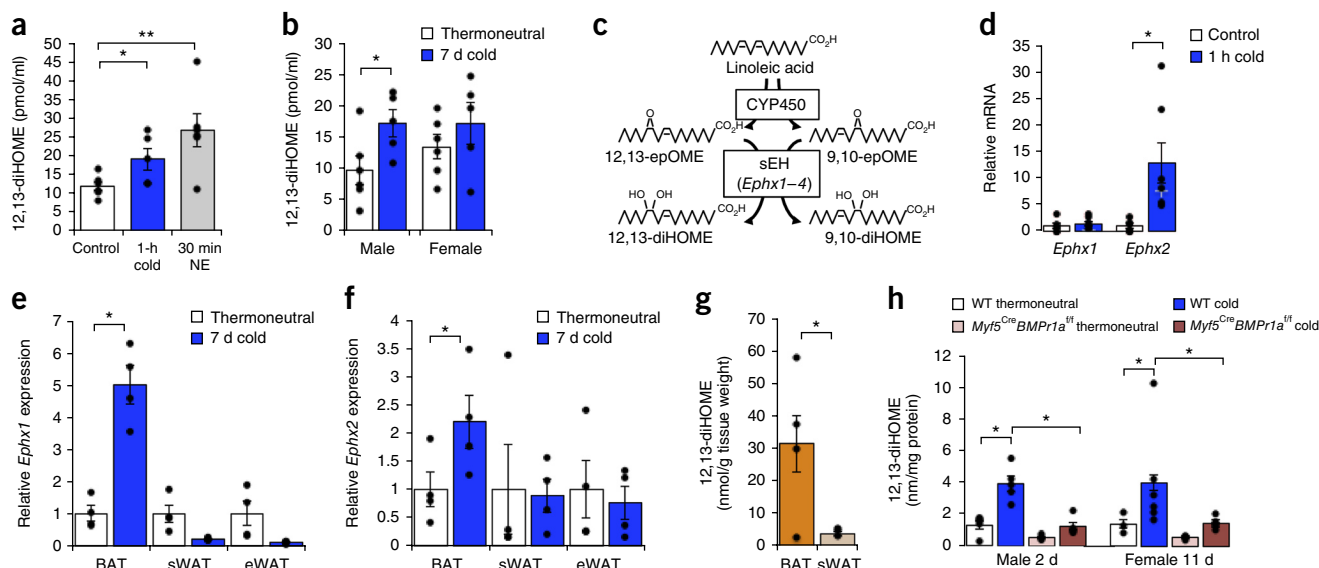
Figure 2 The biosynthetic pathway of 12,13-diHOME is selectively increased in mouse BAT by cold exposure. (**a**) Serum 12,13-diHOME concentration in control mice, as compared to mice treated with norepinephrine (NE) for 30 min, and mice exposed to 4 °C–cold for 1 h. Data are means ± s.e.m.; $n = 6$ control mice, $n = 6$ treated with NE, $n = 5$ exposed to cold. *$P < 0.05$, **$P < 0.005$ by Student's t-test. (**b**) Serum concentration of 12,13-diHOME in male and female mice after a 7-d cold challenge and compared to mice housed at thermoneutrality. Data are means ± s.e.m.; $n = 6$ thermoneutral mice, $n = 5$ cold-exposed mice per group; *$P < 0.05$ by Student's t-test. (**c**) Biosynthetic pathway of 12,13-diHOME production. (**d**) $Ephx1$ and $Ephx2$ mRNA expression measured by qPCR in BAT from control mice as opposed to that in mice exposed to 4 °C–cold for 1 h. Data are means ± s.e.m.; $n = 6$ control mice, $n = 7$ cold-exposed mice. *$P < 0.05$ by Student's t-test. (**e**) $Ephx1$ gene expression, as measured by qPCR in BAT, sWAT and epididymal WAT (eWAT) from mice housed at thermoneutrality or 4 °C–cold for 7 d. Data are presented as normalized means ± s.e.m.; $n = 4$ per group; *$P < 0.05$ by Student's t-test. (**f**) $Ephx2$ gene expression, as measured by qPCR in BAT, sWAT and eWAT of mice housed at either thermoneutrality or cold for 7 d. Data are presented as normalized means ± s.e.m.; $n = 4$ per group; *$P < 0.05$ by Student's t-test. (**g**) 12,13-diHOME concentration in media from BAT and sWAT cultured ex $vivo$ for 1 h, normalized to tissue weight. Data are means ± s.e.m.; $n = 6$ mice; *$P < 0.05$ by Student's t-test. (**h**) 12,13-diHOME concentrations in BAT from wild-type and $Myf5^{Cre}Bmpr1a^{f/f}$ mice housed at cold or thermoneutrality for 2 d or 11 d. Data are plotted as the normalized means ± s.e.m.; $n = 5$ WT thermoneutral males, 5 WT cold-exposed males, 4 $Myf5^{Cre}Bmpr1a^{f/f}$ thermoneutral males, 5 $Myf5^{Cre}Bmpr1a^{f/f}$ cold-exposed males, 3 WT thermoneutral females, 6 WT cold-exposed females, 4 $Myf5^{Cre}Bmpr1a^{f/f}$ thermoneutral females, 6 $Myf5^{Cre}Bmpr1a^{f/f}$ cold-exposed females; *$P < 0.05$ by Student's t-test.

12,13-diHOME was originally identified in mice as a component of the neutrophil oxidative burst[12], but it has not been previously linked to cold stimulation or BAT biology. Biosynthesis of 12,13-diHOME and its isomer 9,10-diHOME begin through the formation of 12,13- or 9,10-epOME epoxides from linoleic acid by cytochrome P450 (Cyp) oxidases, followed by hydrolysis catalyzed by soluble epoxide hydrolases (sEHs) to form the diols 12,13-diHOME and 9,10-diHOME (**Fig. 2c**). Among the four sEH-encoding genes, $Ephx1$ and $Ephx2$ are the major isoforms expressed in adipose tissue[13], and although $Ephx2$-null mice have decreased blood pressure as compared to wild-type mice[14], thermogenic function has not been reported for $Ephx1$-knockout (ref. 15) or $Ephx2$-knockout mice. We found that acute cold exposure (i.e., 1 h) induced a nearly 14-fold increase of $Ephx2$ mRNA levels in the BAT (**Fig. 2d**). Chronic cold exposure (for example, 1 week) also increased both $Ephx1$ (**Fig. 2e**) and $Ephx2$ (**Fig. 2f**) expression only in BAT, and not in other tissues where sEH is expressed (**Supplementary Fig. 4b**). Meta-analysis of publically available data sets profiling gene expression in BAT from mice exposed to cold for different periods of time also consistently showed increased $Ephx2$ expression and differential regulation of several Cyp genes that might participate in this pathway[16–18] in BAT (**Supplementary Fig. 4c**). We detected a high concentration of 12,13-diHOME in adipose tissue (**Supplementary Fig. 4d**), and experiments ex $vivo$ showed that 12,13-diHOME secretion from BAT is higher than that from WAT (**Fig. 2g**).

To further investigate whether BAT or WAT could be a source of 12,13-diHOME upon cold exposure, we used LC–MS/MS to measure

12,13-diHOME in adipose tissue from wild-type and $Myf5^{Cre}Bmpr1a^{f/f}$ mice, the latter of which display a severe defect in classical BAT development and a compensatory browning of subcutaneous WAT (sWAT)[19]. Cold exposure increased local concentrations of 12,13-diHOME in the BAT of WT mice, but not in $Myf5^{Cre}Bmpr1a^{f/f}$ mice (**Fig. 2h**). However, the systemic concentration of 12,13-diHOME in the serum was not different upon cold exposure between WT and $Myf5^{Cre}Bmpr1a^{f/f}$ mice (**Supplementary Fig. 4a**), which suggests that beige fat, which arises in the sWAT as compensation for BAT deficiency in $Myf5^{Cre}Bmpr1a^{f/f}$ mice, might be an appreciable source of this lipokine. Concordantly with these data, 12,13-diHOME was elevated in sWAT from cold-challenged male $Myf5^{Cre}Bmpr1a^{f/f}$ mice with enhanced beige adipogenesis, as compared to wild-type mice housed in cold for 2 d, whereas no effect was observed after 11 d in female mice (**Supplementary Fig. 4e**). Pharmacologic BAT activation using daily treatment with the β3-adrenergic agonist CL316,243 for 10 d increased $Ephx2$ expression in BAT and $Ephx1$ expression in sWAT as compared to vehicle-treated control mice (**Supplementary Fig. 4f,g**), which suggests that 12,13-diHOME can be produced by brown or beige fat in response to β3-adrenergic stimulation. One challenge of understanding the flux of 12,13-diHOME in $vivo$ is that this lipid can be both consumed in the diet and produced in the body, and so further characterization of the biosynthetic pathway will require labeling of 12,13-diHOME itself, and warrants future studies.

To test our initial hypothesis that putative lipokines induced by cold stimulation can facilitate increased thermogenesis, we treated
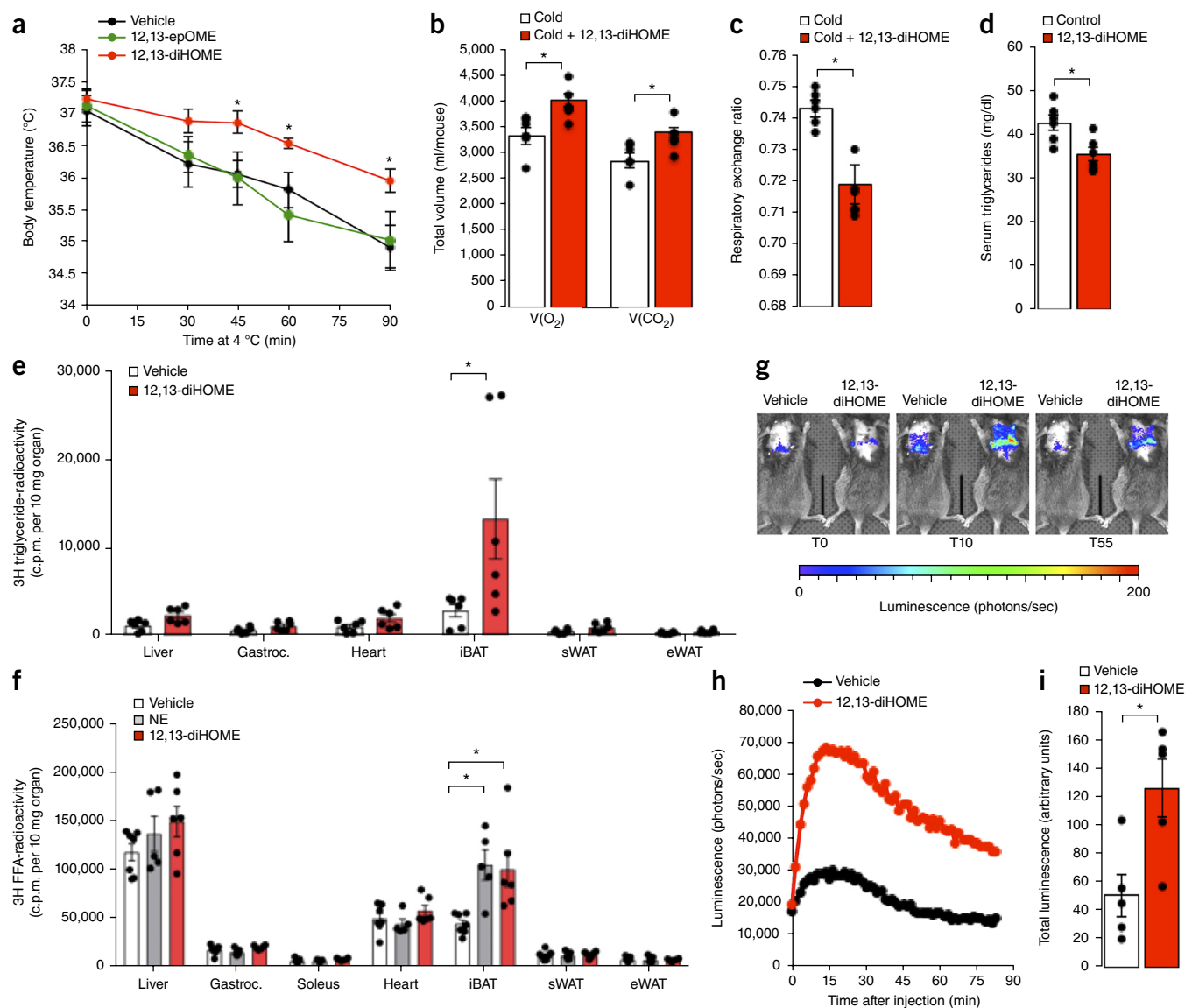
Figure 3 12,13-diHOME enhances cold tolerance and facilitates fatty acid uptake by BAT. (**a**) Body temperature in mice cold challenged at 4 °C for 90 min after pretreatment with 12,13-diHOME, 12,13-epOME or vehicle. Data are means ± s.e.m.; $n = 5$ mice per group; *$P < 0.05$ 12,13-diHOME, as compared to vehicle, by analysis of variance (ANOVA) with *post hoc* Bonferroni test. (**b,c**) Total $V(O_2)$ consumed and $V(CO_2)$ produced (**b**) and average respiratory-exchange ratio (RER, **c**) measurements as measured by Comprehensive Lab Animal Monitoring System (CLAMS) for 1 h of cold (4 °C) in mice acutely treated with 12,13-diHOME or vehicle. Data are means ± s.e.m.; $n = 6$ mice per group; *$P < 0.05$ by Student's t-test. (**d**) Serum triglycerides in mice fed a high-fat diet and treated with 12,13-diHOME or vehicle for 2 weeks. Data are means ± s.e.m.; $n = 5$ treated as compared to $n = 5$ controls; *$P < 0.05$ by Student's t-test. (**e**) Radioactivity per 10 mg of liver, gastrocnemius muscle (Gastroc.), heart, interscapular BAT (iBAT), sWAT and epididymal white adipose tissue (eWAT) from mice treated with vehicle or 12,13-diHOME and then given an oral bolus of ^{3}H-labeled triglyceride. Data are means ± s.e.m.; $n = 6$ per group; *$P < 0.05$ by Student's t-test. (**f**) Radioactivity per 10 mg of tissues from mice treated with vehicle, norepinephrine (NE) or 12,13-diHOME and then given a bolus of ^{3}H-labeled oleate. Data are means ± s.e.m.; $n = 8$ per group; *$P < 0.05$ 12,13-diHOME as compared to vehicle by ANOVA with *post hoc* Bonferroni test. (**g**) Representative images of luciferase activity in *Ucp1*[Cre] *Rosa(stop)Luc* mice injected intravenously with luciferin-conjugated fatty acid and 12,13-diHOME or vehicle. Data are representative images at 0 min, 10 min and 55 min. (**h**) Quantification of luciferase activity in (**g**). (**i**) Total luciferase counts from six individual experiments were averaged and plotted as the normalized means ± s.e.m.; $n = 6$ per group; *$P < 0.05$ 12,13-diHOME as compared to vehicle treatment by Student's t-test.

mice with 12,13-diHOME and measured core body temperature during an acute cold challenge. To minimize cytotoxic effects, we chose to use the dosage of 1 µg/kg with a target concentration of 30–50 nM for *in vivo* administration to mimic the physiologic concentration after cold exposure. This dose is based on the measured circulating concentration of 12,13-diHOME at room temperature and after cold exposure, and it is orders of magnitude lower than the reported concentration that causes lung mitochondrial dysfunction[20].

Importantly, treatment with 12,13-diHOME protected mice from a decrease in body temperature during cold challenge when compared to both vehicle-treated mice and mice injected with the precursor lipid 12,13-epOME (**Fig. 3a**). Of note, except for a transient increase in diastolic pressure, 12,13-diHOME had no effect on blood pressure and pulse (**Supplementary Fig. 5a–c**), which suggests that 12,13-diHOME possesses a therapeutic benefit over sympathomimetics for BAT activation by avoiding potential side effects[21], such
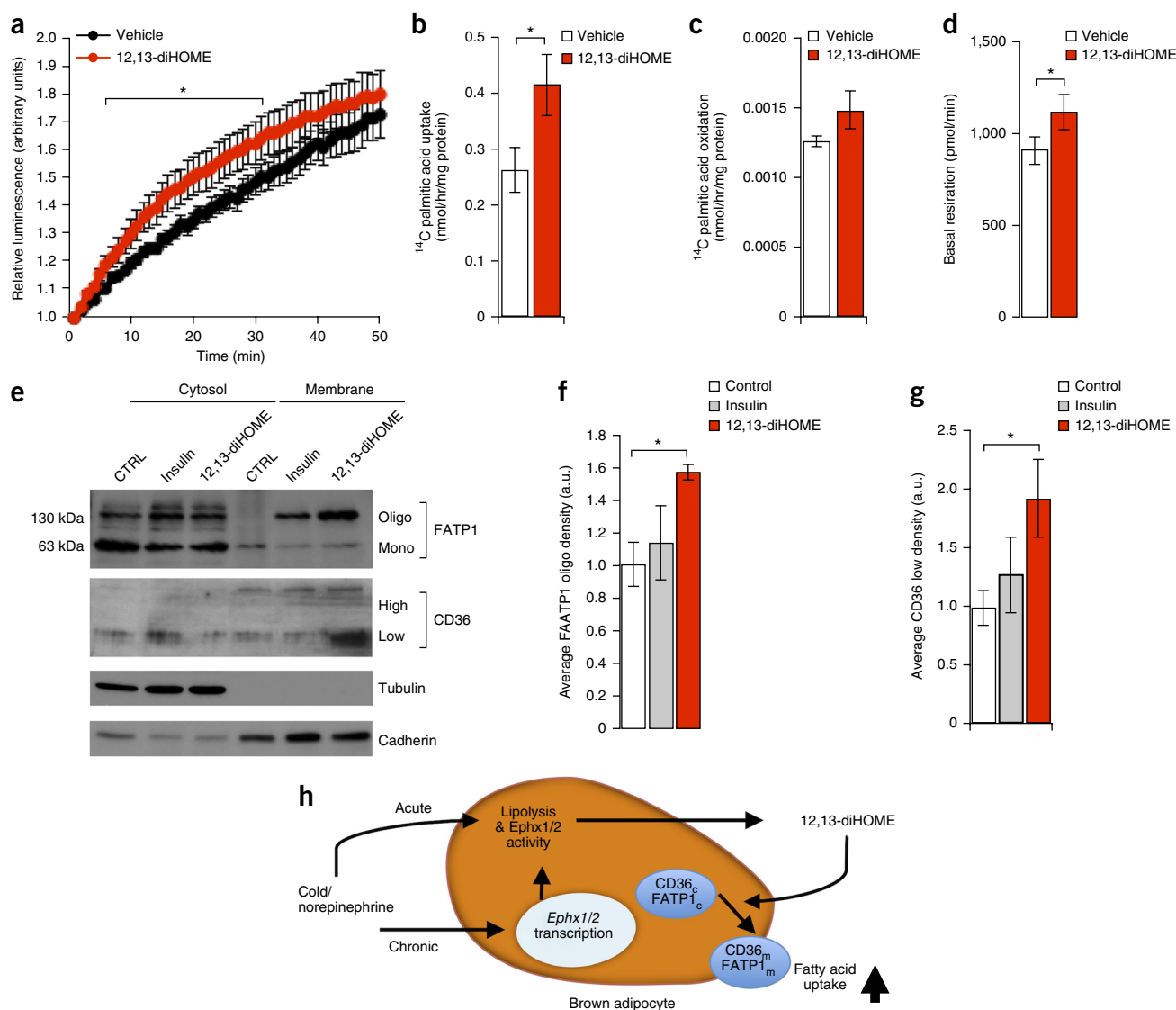
Figure 4 12,13-diHOME promotes fatty acid uptake *in vitro* by activating the translocation and oligomerization of FA transporters. (**a**) Fatty acid uptake in mature brown adipocytes constitutively expressing firefly luciferase that were pretreated with either 12,13-diHOME or vehicle, as measured by luciferase activity using 10 μM FFA-SS-Luc. Data are plotted as the normalized means ± s.e.m.; $n = 6$ technical-replicate wells per group; *$P < 0.05$ 12,13-diHOME as compared to vehicle by ANOVA with *post hoc* Bonferroni test. (**b**) Radiolabeled ^{14}C palmitic acid uptake in mature brown adipocytes pretreated for 15 min with either 12,13-diHOME or vehicle. The data were normalized by protein content. Data are presented as means ± s.e.m.; $n = 10–11$ technical-replicate wells per group; *$P < 0.05$ 12,13-diHOME as compared to vehicle by Student's *t*-test. (**c**) Radiolabeled ^{14}C palmitic acid oxidation in mature brown adipocytes pretreated with either 12,13-diHOME or vehicle. The data were normalized by protein content. Data are presented as means ± s.e.m.; $n = 10–11$ technical-replicate wells per group. (**d**) Basal respiration of mature brown adipocytes treated with either 12,13-diHOME or vehicle. The data were normalized by protein content. Data are presented as means ± s.e.m.; $n = 10–11$ technical-replicate wells per group; *$P < 0.05$ 12,13-diHOME as compared to vehicle by Student's *t*-test. (**e**) Western blot analysis of membrane and cytosol fractions of differentiated brown adipocytes treated with 12,13-diHOME or vehicle. Data are presented as a representative image; $n = 3$ separate experiments. (**f**) The upper band corresponding to the oligomer form of FATP1 was measured by densitometry from immunoblots of three independent experiments. Data are presented as means ± s.e.m.; $n = 3$ separate experiments; *$P < 0.05$ 12,13-diHOME as compared to vehicle by one-way ANOVA. (**g**) Densitometry of the low-glycosylation form of CD36 from immunoblots of three independent experiments. Data are presented as means ± s.e.m.; $n = 3$ separate experiments; *$P < 0.05$ 12,13-diHOME as compared to vehicle by one-way ANOVA. (**h**) Proposed model of 12,13-diHOME biosynthesis and action in cold-activated BAT.

as tachycardia or hypertension. Consistently with these findings, 12,13-diHOME-treated animals displayed increased oxygen consumption and carbon dioxide production in the cold as compared to vehicle-treated mice (**Fig. 3b**). These changes result in a decreased respiratory exchange ratio (**Fig. 3c**), which indicates increased lipid oxidation and further suggests that the effect of 12,13-diHOME on BAT metabolism is mediated, at least in part, through enhanced lipid metabolism.

To test therapeutic applications of 12,13-diHOME, we treated mice with diet-induced obesity with 12,13-diHOME daily for 2 weeks at 10 μg/kg body weight. Although no effects on body weight, glucose tolerance or circulating nonesterified FA (**Supplementary Fig. 6a–c**) were observed at this dose, 12,13-diHOME decreased circulating triglycerides (**Fig. 3d**) and increased expression of lipoprotein lipase (*LPL*) in BAT, suggesting increased hydrolysis of triglycerides[22,23] (**Supplementary Fig. 6d**). These results, taken together with

well-supported reports that activated BAT takes up large quantities of FA from circulating triglyceride-rich lipoproteins[23–27], led us to test the effects of 12,13-diHOME on lipid uptake *in vivo*. Because 12,13-diHOME decreased circulating triglycerides levels and the principal source of FA *in vivo* is in the form of triglycerides packaged into lipoproteins, we measured the effect of 12,13-diHOME on the uptake of radiolabeled triglycerides delivered by oral gavage (**Fig. 3e**). Indeed, mice treated with 12,13-diHOME exhibited increased BAT-specific lipid uptake and improved oral lipid tolerance (**Supplementary Fig. 6e**). Similarly, 12,13-diHOME increased radiolabeled FA uptake (**Fig. 3f**) and glucose uptake (**Supplementary Fig. 6f**) specifically into the BAT, similar to a level achieved by NE stimulation.

Given the fast and dynamic nature of FA uptake, we sought to monitor 12,13-diHOME-stimulated fatty acid uptake in real time. We generated transgenic mice expressing firefly luciferase specifically in brown adipocytes (*Ucp1*[Cre] *Rosa(stop)Luc*). We injected these mice intravenously with FFA-SS-Luc, a fatty acid–luciferin conjugate that follows the uptake of natural FA and releases luciferin only after internalization[28]. In this model, luciferase is expressed exclusively in UCP1-expressing adipocytes, so the luciferin substrate can be oxidized only in these cells to release light to measure brown adipocyte FA uptake (**Fig. 3g** and **Supplementary Video 1**). Mice treated with 12,13-diHOME, as compared to vehicle-treated animals, had an increased luminescence signal for BAT that was both rapid and sustained over the course of the experiment (**Fig. 3h,i**). Taken together, these data demonstrate a prothermogenic effect of 12,13-diHOME that is linked to acute, BAT-specific FA uptake.

To identify potential cell-autonomous mechanisms for increased FA uptake in BAT, we tested the effects of 12,13-diHOME on brown adipocytes constitutively expressing luciferase *in vitro*. In agreement with experiments *in vivo*, FFA-SS-Luc uptake *in vitro* was also increased by 12,13-diHOME treatment (**Fig. 4a** and **Supplementary Video 2**), whereas no additive effect of NE treatment was observed (data not shown), which suggests that 12,13-diHOME might act downstream of NE. Similarly, 12,13-diHOME markedly increased radiolabeled FA uptake in brown adipocytes, with an increase in FA oxidation that did not reach statistical significance (**Fig. 4b,c**). As a result of consuming the FA fuel, basal respiration was increased in 12,13-diHOME-treated brown adipocytes (**Fig. 4d**), but there was no effect on maximal respiratory capacity or uncoupling. Taken together with the *in vivo* data (**Fig. 3b,c**), these findings indicate that the effect of 12,13-diHOME was due primarily to increased metabolic flux and fuel consumption.

In adipocytes, FA uptake is mediated in part by a diverse family of FA transport proteins, including CD36 and fatty acid transport protein 1 (FATP1), both of which are hormone-sensitive FA transporters[26,29] required for nonshivering thermogenesis in mice[30,31]. Membrane translocation of both the low-glycosylation form of CD36 (ref. 26) and oligomeric FATP1 (ref. 32) is robustly induced by 12,13-diHOME, consistent with increased FA uptake (**Fig. 4e–g**; uncropped versions of the western blots are in **Supplementary Fig. 7**). Fractionation of cellular compartments was confirmed by using tubulin as a marker of cytosol and cadherin to mark the membrane.

Taken together, these results lead us to propose a model (**Fig. 4h**) wherein cold exposure activates the production of 12,13-diHOME in BAT tissue by increasing lipolysis to provide substrates for sEH and increasing sEH gene expression, ultimately leading to increased circulating 12,13-diHOME. 12,13-diHOME acts, at least in part, through an autocrine–paracrine mechanism to activate FA-transporter translocation in brown adipocytes, which leads to increased FA uptake and triglyceride clearance and thus facilitates thermogenesis by providing fuel.

Chronic cold exposure further increases gene expression of sEH, specifically in brown or beige adipocytes, to increase biosynthesis of 12,13-diHOME. Notably, even metabolically inert FAs are known to activate UCP1 directly (ref. 33), and the direct effects of 12,13-diHOME on UCP1-mediated uncoupling require further investigation. Our experiments *in vivo*, however, supported a direct effect of 12,13-diHOME on FA uptake.

On the basis of our model, 12,13-diHOME facilitates BAT thermogenic activity by selectively promoting fuel uptake, which suggests potential applications for the treatment of hyperlipidemia. Indeed, acute 12,13-diHOME treatment protected mice from the effects of cold challenge, and chronic treatment (i.e., 2 weeks) of mice with diet-induced obesity with 12,13-diHOME resulted in a reduction of circulating triglyceride levels without alteration of body weight. These data point to a complex fuel-consumption and refueling process that affects energy balance during cold exposure, and presumably, upon 12,13-diHOME treatment. In cold conditions, fatty acids in brown adipocytes serve as both fuels to be oxidized for thermoregulation and as substrates for the biosynthesis of 12,13-diHOME. Because 12,13-diHOME activates FA uptake, the consumption of cellular fuel is coupled to a potent and specific refueling signal. By identifying this mechanism of BAT-specific lipid utilization, it might be possible to unlock the maximum therapeutic potential of brown fat in humans.

METHODS

Methods, including statements of data availability and any associated accession codes and references, are available in the online version of the paper.

Note: Any Supplementary Information and Source Data files are available in the online version of the paper.

AUTHOR CONTRIBUTIONS
M.D.L. designed research, carried out experiments, analyzed data and wrote the paper. L.O.L. carried out fatty acid uptake *in vitro* and Seahorse assays. M.L. carried out translocation assays. A.B., A.L. and C.S. carried out fatty acid–, triglyceride- and glucose-uptake assays *in vivo*. F.S. and T.L.H. performed gene-expression analysis and immunoblotting. H.T. carried out fatty acid–uptake assays *in vitro*. M.F.H., L.A.B. and F.J.M. carried out *in vivo* experiments. F.G., N.R.N. and M.A.K. oversaw lipidomics experiments. E.Y.C. performed lipidomic experiments and analyzed data. A.M.C. designed research and carried out human cold-exposure experiments. M.B. provided human plasma from well-phenotyped human individuals for 12,13-diHOME measurements. L.J.G. oversaw FA-uptake experiments. G.S.H. oversaw tracer-uptake experiments *in vivo*. K.I.S. oversaw *in vivo* experiments and analyzed data. M.D.L. and Y.-H.T. directed the research and co-wrote the paper.

Reprints and permissions information is available online at http://www.nature.com/reprints/index.html.

1. Townsend, K. & Tseng, Y.H. Brown adipose tissue: Recent insights into development, metabolic function and therapeutic potential. *Adipocyte* **1**, 13–24 (2012).
2. Lynes, M.D. & Tseng, Y.H. Unwiring the transcriptional heat circuit. *Proc. Natl. Acad. Sci. USA* **111**, 14318–14319 (2014).
3. Romu, T. *et al.* A randomized trial of cold-exposure on energy expenditure and supraclavicular brown adipose tissue volume in humans. *Metabolism* **65**, 926–934 (2016).
4. Schellen, L., Loomans, M.G., de Wit, M.H., Olesen, B.W. & van Marken Lichtenbelt, W.D. The influence of local effects on thermal sensation under non-uniform environmental conditions—gender differences in thermophysiology, thermal comfort and productivity during convective and radiant cooling. *Physiol. Behav.* **107**, 252–261 (2012).
5. Hanssen, M.J. *et al.* Short-term cold acclimation improves insulin sensitivity in patients with type 2 diabetes mellitus. *Nat. Med.* **21**, 863–865 (2015).
6. Cao, H. *et al.* Identification of a lipokine, a lipid hormone linking adipose tissue to systemic metabolism. *Cell* **134**, 933–944 (2008).
7. Liu, S. *et al.* A diurnal serum lipid integrates hepatic lipogenesis and peripheral fatty acid use. *Nature* **502**, 550–554 (2013).
8. Yore, M.M. *et al.* Discovery of a class of endogenous mammalian lipids with anti-diabetic and anti-inflammatory effects. *Cell* **159**, 318–332 (2014).
9. Cypess, A.M. *et al.* Cold but not sympathomimetics activates human brown adipose tissue in vivo. *Proc. Natl. Acad. Sci. USA* **109**, 10001–10005 (2012).
10. Oh, D.Y. *et al.* GPR120 is an omega-3 fatty acid receptor mediating potent anti-inflammatory and insulin-sensitizing effects. *Cell* **142**, 687–698 (2010).
11. Hoene, M. *et al.* The lipid profile of brown adipose tissue is sex-specific in mice. *Biochim. Biophys. Acta* **1841**, 1563–1570 (2014).
12. Thompson, D.A. & Hammock, B.D. Dihydroxyoctadecamonoenoate esters inhibit the neutrophil respiratory burst. *J. Biosci.* **32**, 279–291 (2007).
13. Su, A.I. *et al.* A gene atlas of the mouse and human protein-encoding transcriptomes. *Proc. Natl. Acad. Sci. USA* **101**, 6062–6067 (2004).
14. Sinal, C.J. *et al.* Targeted disruption of soluble epoxide hydrolase reveals a role in blood pressure regulation. *J. Biol. Chem.* **275**, 40504–40510 (2000).
15. Miyata, M. *et al.* Targeted disruption of the microsomal epoxide hydrolase gene. Microsomal epoxide hydrolase is required for the carcinogenic activity of 7,12-dimethylbenz[a]anthracene. *J. Biol. Chem.* **274**, 23963–23968 (1999).
16. Marcher, A.B. *et al.* RNA-seq and mass-spectrometry-based lipidomics reveal extensive changes of glycerolipid pathways in brown adipose tissue in response to cold. *Cell Rep.* **13**, 2000–2013 (2015).
17. Hao, Q. *et al.* Transcriptome profiling of brown adipose tissue during cold exposure reveals extensive regulation of glucose metabolism. *Am. J. Physiol. Endocrinol. Metab.* **308**, E380–E392 (2015).
18. Rosell, M. *et al.* Brown and white adipose tissues: intrinsic differences in gene expression and response to cold exposure in mice. *Am. J. Physiol. Endocrinol. Metab.* **306**, E945–E964 (2014).
19. Schulz, T.J. *et al.* Brown-fat paucity due to impaired BMP signalling induces compensatory browning of white fat. *Nature* **495**, 379–383 (2013).
20. Sisemore, M.F. *et al.* Cellular characterization of leukotoxin diol-induced mitochondrial dysfunction. *Arch. Biochem. Biophys.* **392**, 32–37 (2001).
21. Redman, L.M. *et al.* Lack of an effect of a novel β3-adrenoceptor agonist, TAK-677, on energy metabolism in obese individuals: a double-blind, placebo-controlled randomized study. *J. Clin. Endocrinol. Metab.* **92**, 527–531 (2007).
22. Klingenspor, M. *et al.* Multiple regulatory steps are involved in the control of lipoprotein lipase activity in brown adipose tissue. *J. Lipid Res.* **37**, 1685–1695 (1996).
23. Bartelt, A. *et al.* Brown adipose tissue activity controls triglyceride clearance. *Nat. Med.* **17**, 200–205 (2011).
24. Berbée, J.F. *et al.* Brown fat activation reduces hypercholesterolaemia and protects from atherosclerosis development. *Nat. Commun.* **6**, 6356 (2015).
25. Khedoe, P.P. *et al.* Brown adipose tissue takes up plasma triglycerides mostly after lipolysis. *J. Lipid Res.* **56**, 51–59 (2015).
26. Schlein, C. *et al.* FGF21 lowers plasma triglycerides by accelerating lipoprotein catabolism in white and brown adipose tissues. *Cell Metab.* **23**, 441–453 (2016).
27. Warner, A. *et al.* Activation of β3-adrenoceptors increases *in vivo* free fatty acid uptake and utilization in brown but not white fat depots in high-fat fed rats. *Am. J. Physiol. Endocrinol. Metab.* **311**, E901–E910 (2016).
28. Henkin, A.H. *et al.* Real-time noninvasive imaging of fatty acid uptake in vivo. *ACS Chem. Biol.* **7**, 1884–1891 (2012).
29. Stahl, A., Evans, J.G., Pattel, S., Hirsch, D. & Lodish, H.F. Insulin causes fatty acid transport protein translocation and enhanced fatty acid uptake in adipocytes. *Dev. Cell* **2**, 477–488 (2002).
30. Wu, Q. *et al.* Fatty acid transport protein 1 is required for nonshivering thermogenesis in brown adipose tissue. *Diabetes* **55**, 3229–3237 (2006).
31. Putri, M. *et al.* CD36 is indispensable for thermogenesis under conditions of fasting and cold stress. *Biochem. Biophys. Res. Commun.* **457**, 520–525 (2015).
32. Richards, M.R. *et al.* Oligomerization of the murine fatty acid transport protein 1. *J. Biol. Chem.* **278**, 10477–10483 (2003).
33. Shabalina, I.G., Kalinovich, A.V., Cannon, B. & Nedergaard, J. Metabolically inert perfluorinated fatty acids directly activate uncoupling protein 1 in brown-fat mitochondria. *Arch. Toxicol.* **90**, 1117–1128 (2016).

ONLINE METHODS

General experimental approaches. No samples, mice, human individuals or data points were excluded from the reported analyses. Samples were not randomized to experimental groups. Analyses were not performed in a blinded fashion except as noted below.

Human participants. Human plasma was acquired from a previously performed cold-exposure experiment approved by the Human Studies Institutional Review Boards of Beth Israel Deaconess Medical Center[9]. All individuals gave written informed consent before taking part in the study. Briefly, nine healthy volunteers participated in three separate, independent study visits conducted in random order on the basis of a Latin-square design. The night before the study day, participants were admitted to the clinical research center, and they began fasting from 12:00 a.m. onward. Room temperature was maintained above 23 °C throughout the stay in the clinical research center. Upon waking the next morning, the volunteers put on a standard hospital scrub suit. Depending on the study day, one of three stimuli was given: a single intramuscular dose of ephedrine 1 mg/kg; an equal volume of saline; or the volunteer was transported to a room set to 20 °C and donned a surgeon's cooling vest (Polar Products) with the water temperature set to 14 °C that was monitored by a digital thermometer (Fisher Scientific). 60 min after the injection of ephedrine, saline or the initiation of cold exposure, blood was drawn for the measurement of lipid levels, and then an intravenous bolus of 440 MBq (12 mCi) of ^{18}F-FDG was administered. 60 min after the ^{18}F-FDG injection, images were acquired using a Discovery LS multidetector helical PET-CT scanner (GE Medical Systems). BAT mass and activity were both quantified using the PET-CT Viewer shareware.

For the second cohort of human participants, 55 individuals were selected from the Leipzig biobank (42 women and 13 men) to represent a wide range of BMI (17.5–75.4 kg/m^2), categories of lean (BMI < 25 kg/m^2; $n = 15$; 4 male (M)/11 female (F)), overweight (BMI 25.1–29.9 kg/m^2; $n = 13$; 4 M/9 F) or obese (BMI > 30 kg/m^2; $n = 27$; 5 M/22 F) and glucose-metabolism parameters (fasting plasma glucose 3.9–13.4 mmol/liter; fasting plasma insulin 3.8–451 pmol/liter, HOMA-IR: 0.1–25). In the subgroup of lean, all individuals were normal glucose tolerant (NGT), whereas in the overweight subgroup, 10 individuals with NGT and 3 with type 2 diabetes (T2D), and in the obese group, 20 NGT individuals and 7 individuals with T2D were included. Phenotyping, definition of NGT and T2D, as well as analyses of serum/plasma parameters (fasting plasma insulin (FPI), fasting plasma glucose (FPG), hemoglobin A1c (HbA1c), C-reactive protein (CrP), leptin, total cholesterol, aspartate transaminase (ASAT) and γ-glutamyl transpeptidase (gGT) serum concentrations) were performed, as described previously[35]. Collection of human biomaterial, serum analyses and phenotyping were approved by the ethics committee of the University of Leipzig (approval numbers: 159-12-21052012 and 017-12-23012012), and all individuals gave written informed consent before taking part in the study.

Lipidomic profiling and 12,13-diHOME quantification. All lipid standards were purchased from the Cayman Chemical Company, Avanti Polar Lipids or Santa Cruz Biotechnology. C$_{18}$SPE cartridges were purchased from Biotage. All solvents are of high-performance liquid chromatography (HPLC). or LC–MS/MS grade and were acquired from Sigma-Aldrich, Fisher Scientific or VWR International. Tissue samples were homogenized in 0.1× PBS in Omni homogenizing tubes with ceramic beads at 4 °C. Aliquots of 100 µl serum or 1 mg protein of homogenized tissue measured by the Pierce BCA kit (Life Technologies) were taken, depending on the experiment. A mixture of deuterium-labeled internal standards was added to each aliquot, followed by 3× volume of a sample of cold methanol (MeOH). Samples were vortexed for 5 min and stored at −20 °C overnight. Cold samples were centrifuged at 14,000g for 10 min, and the supernatant was then transferred to a new tube, and 3 ml of acidified H$_2$O (pH 3.5) was added to each sample before C$_{18}$ SPE and performed as previously described[36]. The methyl formate fractions were collected, dried under nitrogen and reconstituted in 50 µl MeOH:H$_2$O (1:1, by volume). Samples were transferred to 0.5 ml tubes and centrifuged at 20,000g at 4 °C for 10 min. 35 µl of supernatant was transferred to LC–MS/MS vials for analysis using the BERG LC–MS/MS-mediator lipidomics platform. Separation of signaling lipids was performed on an Ekspert MicroLC 200

system (Eksigent Technologies) with a Synergi Fusion-RP capillary C$_{18}$ column (150 × 0.5 mm, 4 µm; Phenomenex) heated to 40 °C. A sample volume of 10 µl was injected at a flow rate of 20 µl/min. Lipids were separated using mobile phases A (100% H$_2$O, 0.1% acetic acid) and B (100% MeOH, 0.1% acetic acid) with a gradient starting at 60% B for 0.5 min, steadily increasing to 80% B by 5 min, reaching 95% B by 9 min, holding for 1 min and then decreasing to 60% B by 12 min. MS analysis was performed on a SCIEX TripleTOF 5600+ system using the HR-MRM strategy consisting of a time of flight (TOF) MS experiment looped with multiple MS/MS experiments. MS spectra were acquired in high-resolution mode (>30,000) using a 100-ms accumulation time per spectrum. Full-scan MS/MS was acquired in high-sensitivity mode, with an accumulation time optimized per cycle. Collision energy was set using rolling collision energy with a spread of 15 V. The identity of a component was confirmed using PeakView software (SCIEX), and quantification was performed using MultiQuant software (SCIEX). The quantification of 12,13-diHOME was performed against a standard calibration curve built with five points ranging from 0.01 pg/µl to 100 pg/µl. Obtained values were corrected with the corresponding internal standard d$_4$-9,10-diHOME. All measurements were performed in a blinded fashion.

Mice and treatments. All animal procedures were approved by the Institutional Animal Use and Care Committee at Joslin Diabetes Center and Harvard T.H. Chan School of Public Health. For the cold-exposure experiments, radiolabeled FA-uptake experiment, and diet-induced obesity experiment, 12-week-old male C57BL/6J mice (stock no. 000664) were purchased from the Jackson Laboratory. For acute BAT activation, mice were either killed as control animals, treated with NE for 30 min or placed at 4 °C for 1 h, then killed for serum and tissue collection. In chronic cold exposures, transgenic mice carrying floxed alleles for the BMP receptor 1A were used to generate conditional gene-deletion mouse models by intercrossing with *Myf5*-driven Cre recombinase and as compared to Cre-negative littermate controls as described previously[19]. In addition to C57BL/6J mice, these transgenic animals were used for all chronic-cold-exposure experiments, with mice 10–18 weeks of age housed in a temperature-controlled diurnal incubator (Caron Products & Services) at either 4 °C (cold) or 30 °C (thermoneutrality) on a 12-h light–dark cycle. In all experiments, interscapular BAT, inguinal sWAT and serum were dissected after euthanization.

For *ex vivo* tissue-incubation experiments, interscapular BAT and inguinal sWAT were dissected from 12-week-old male C57BL/6J mice and incubated at 37 °C in Krebs solution for 1 h, after which the tissue was discarded and LC–MS/MS was performed on the conditioned Krebs solution.

For cold-tolerance assay, mice were injected retro-orbitally with 1 µg/kg body weight 12,13-diHOME in 0.1% w/v BSA in PBS or vehicle and then immediately placed in a cold room maintained at 4 °C and body-core temperature was determined by rectal-probe measurements. Mice injected retro-orbitally were also used to measure blood pressure and pulse with the tail-cuff method (Hatteras Instruments).

For *in vivo* triglyceride organ-uptake studies, mice were orally gavaged with 10 ml/kg olive oil (Sigma-Aldrich) containing [9,10-^{3}H(N)]-triolein (PerkinElmer, 0.3 mCi/kg) 15 min after treatment with either vehicle, 1 µg/kg body weight 12,13-diHOME in 0.1% BSA PBS. Similarly, an oleate/^{3}H-oleate tracer mix was complexed to fatty acid–free BSA[26] and injected into the tail vein of wild-type C57BL/6J mice 15 min after treatment with either vehicle, 1 µg/kg body weight 12,13-diHOME in 0.1% BSA PBS or NE. Glucose-uptake studies were also performed by injection into the tail vein with 2-desoxy-D-[^{14}C] -glucose (PerkinElmer, 0.025 mCi per kg) in PBS 15 min after treatment with either vehicle, 1 µg/kg body weight 12,13-diHOME in 0.1% BSA PBS or NE. In all assays, organs were harvested after 15 min of radiotracer uptake under terminal anesthesia and systemic perfusion with PBS-heparin (10 U/ml) via the left heart ventricle. Tissues were homogenized by using Solvable (PerkinElmer), and disintegrations per minute per organ data were calculated by scintillation counting.

For *in vivo* bioluminescent fatty acid–uptake experiments, *Ucp1*^{Cre} mice (stock no. 024670) were bred with *Rosa(stop)Luc* mice (stock no. 005125), both obtained from the Jackson Laboratory. Male offspring carrying the *Ucp1*^{Cre} allele were injected retro-orbitally with 1 ug/kg body weight 12,13-diHOME in 0.1% BSA PBS or vehicle, and all mice were co-injected with 2 µm FFA-SS-Luc

(Intrace Medical). Mice were anesthetized with isofluorane and imaged using the IVIS Spectrum CT using sequential 30 s exposures for 1 h. Data was analyzed using Living Image Software, and movies were assembled from individual images using ImageJ.

For CLAMS studies, mice were injected intravenously with 1 µg/kg body weight 12,13-diHOME in 0.1% BSA PBS or vehicle and then monitored using the CLAMS system in cold conditions (4 °C) for 1 h. Respiratory-exchange ratio (RER) was calculated as the ratio of total carbon dioxide produced to total oxygen consumed.

For the experiments with daily injections of 12,13-diHOME, mice were fed with a high-fat diet containing 60 kcal% fat (Research Diets stock no. D12492) for 16 weeks before treatment and during the course of the experiment. Mice were first injected intraperitoneally daily with 1 µg/kg body weight, 13-diHOME in 0.1% BSA w/v in PBS or vehicle and body for 1 week, and then injected every day with 10 µg/kg body weight for 2 weeks. For all experiments, serum was collected and triglycerides were measured using a standard enzymatic assay (ZenBiosystems). Nonesterified FAs were also measured using a colorimetric assay (Wako Chemicals USA). High-density- and low-density-lipoprotein fractions were isolated, and cholesterol was measured using a colorimetric assay (Abcam). All mice were allowed *ad libitum* access to water and food.

mRNA expression. Total RNA was extracted from tissue with Trizol and purified using a spin-column kit (Zymo Research). RNA (from 500 ng to 1 µg) was reverse transcribed with a high-capacity complementary DNA (cDNA) reverse-transcription kit (Applied Biosystems). Real-time PCR was performed in mouse tissues, starting with 10 ng of cDNA and forward and reverse oligonucleotide primers (300 nM each) in a final volume of 10 µl with SYBR green PCR Master Mix (Roche). Fluorescence was determined and analyzed in an ABI Prism 7900-sequence detection system (Applied Biosystems). Acidic ribosomal phosphoprotein P0 (ARBP) expression was used to normalize gene expression. Real-time PCR primer sequences are listed in **Supplementary Table 3**.

In vitro lipid assays. Stromal vascular cells were isolated from interscapular BAT dissected from TgLuc mice (stock no. 008450) obtained from the Jackson Laboratory. Cells were immortalized and differentiated into adipocytes *in vitro* according to the protocol described in ref. 34. After 1 h of serum starvation, mature adipocytes were treated with 1 µM 12,13-diHOME or methyl acetate as vehicle in 0.1% w/v BSA in PBS for 15 min. After this treatment, cells were incubated with 10 µm FFA-SS-Luc (Intrace Medical) and imaged using the IVIS Spectrum CT using sequential 30-s exposures for 1 h. Data was analyzed using Living Image Software, and movies were assembled from individual images using ImageJ. All cultures were confirmed to be mycoplasma free.

FA uptake and oxidation were determined by measuring both ^{14}C-labeled palmitic acid uptake and conversion of ^{14}C-labeled palmitic acid into CO_2. Brown preadipocytes were differentiated according to a standard adipogenic differentiation protocol for 9 d before cells were serum starved for 1 h. Cells were treated with 1 µM 12,13-diHOME or methyl acetate as vehicle in 0.1% w/v BSA in PBS for 15 min before the culture medium was removed, and cells were incubated with DMEM/H containing 4% FA-free BSA w/v in PBS, 0.5 mM palmitic acid, and 0.2 µCi/mL [1-^{14}C]-palmitic acid (PerkinElmer Life and Analytical Science, Waltham, MA) for 1 h. The incubation medium was transferred to a vial containing 1-M acetic acid, capped quickly and allowed to incubate for 1 h for CO_2 gas to be released[14]. The CO_2 released was absorbed by hyamine hydroxide, and activity was counted. FA oxidation was calculated from CO_2 generated. To measure fatty acid uptake, cells were rinsed twice with PBS and lysed after incubation with [1-^{14}C]-palmitic acid. Lipids were extracted using a chloroform-methanol mixture (2:1), and ^{14}C-counts were determined in the organic phase. Protein concentrations were determined by using the Pierce BCA kit (Life Technologies) according to instructions, and FA uptake (^{14}C lipids in the cells) and oxidation ($^{14}CO_2$ generated) were normalized to protein content. All cells were confirmed to be mycoplasma free.

Seahorse bioanalyzer. Brown preadipocytes were seeded onto gelatin-coated Seahorse Plates and differentiated according to standard protocols. Cells were starved for 1 h and then treated for 15 min with 1 µM 12,13-diHOME or methyl acetate as vehicle. The oxygen-consumption rates (OCR) were monitored in 200 µM palmitic acid plus 100 µM albumin in a Seahorse XF24 instrument using the standard protocol of 3-min mix, 2-min wait and 3-min measure. For the normalization of respiration to protein content, cells were lysed in RIPA buffer and protein concentration was measured using the Pierce BCA kit (Life Technologies).

Membrane fractionation. Brown preadipocytes were differentiated according to a standard adipogenic differentiation protocol for 9 d before cells were serum starved for 1 h. Cells were treated with 1 µM 12,13-diHOME or methyl acetate as vehicle in 0.1% BSA w/v in PBS for 15 min before cells were scraped from tissue-culture plates into homogenization buffer and membranes were separated according to previously published protocols[37]. Protein lysates were stored at −20 °C until further use. Protein concentrations were determined by using the Pierce BCA kit (Life Technologies), according to the manufacturer's instructions. For immunoblots, lysates were diluted into Laemmli buffer and boiled and then loaded onto 10% Tris gels for SDS–PAGE. After complete separation of the proteins, these were transferred on a PVDF membrane (Amersham Biosciences) and blocked in western blocking buffer (Roche), and primary antibodies (**Supplementary Table 4**) were applied in blocking buffer over night at 4 °C. After washing 4× for 15 min with TBS-T, secondary antibodies were applied for 1 h in blocking buffer. Membranes were washed again 3× times for 15 min in TBS-T and developed using chemiluminescence (ThermoFisher). After scanning films, densitometry was analyzed using ImageJ software. All antibodies are listed in **Supplementary Table 4**.

Statistics. All statistics were calculated using Microsoft Excel, Graphpad Prism and RStudio using LIMMA package. In all cases, we assumed equal variance. For consistency, the Spearman correlation coefficient is shown; however, all Pearson and Kendall coefficients reached similar levels of significance. For all correlation coefficients, the *P* value was calculated using algorithm AS 89 (ref. 38). No statistical method was used to predetermine sample size. The experiments were not randomized or blinded.

Data-availability statement. All data underlying the findings reported in this manuscript are provided as part of the article. Source data are available online for **Figures 1–4**.

34. Tseng, Y.H., Kriauciunas, K.M., Kokkotou, E. & Kahn, C.R. Differential roles of insulin receptor substrates in brown adipocyte differentiation. *Mol. Cell. Biol.* **24**, 1918–1929 (2004).
35. Klöting, N. *et al.* Insulin-sensitive obesity. *Am. J. Physiol. Endocrinol. Metab.* **299**, E506–E515 (2010).
36. Powell, W.S. Extraction of eicosanoids from biological fluids, cells, and tissues. *Methods Mol. Biol.* **120**, 11–24 (1999).
37. Nishiumi, S. & Ashida, H. Rapid preparation of a plasma membrane fraction from adipocytes and muscle cells: application to detection of translocated glucose transporter 4 on the plasma membrane. *Biosci. Biotechnol. Biochem.* **71**, 2343–2346 (2007).
38. Best, D.J. & Roberts, D.E. The upper tail probabilities of Spearman's *Rho. Appl. Stat.* **24**, 377–379 (1975).